The Journal of Experimental Biology 207, 3639-3648
Published by The Company of Biologists 2004
doi:10.1242/jeb.01182



# Determination of peak vertical ground reaction force from duty factor in the horse (*Equus caballus*)

T. H. Witte[1], K. Knill[1] and A. M. Wilson[1,2,*]

[1]*Structure and Motion Lab, The Royal Veterinary College, Hawkshead Lane, Hatfield, Hertfordshire, AL9 7TA, UK* and [2]*Structure and Motion Lab, University College London, Royal National Orthopaedic Hospital, Brockley Hill, Stanmore, Middlesex, HA7 4LP, UK*

*Author for correspondence (e-mail: awilson@rvc.ac.uk)

*Accepted 13 July 2004*

**Summary**

**Measurement of peak vertical ground reaction force (GRFz) from multiple limbs simultaneously during high-speed, over-ground locomotion would enhance our understanding of the locomotor mechanics of cursorial animals. Here, we evaluate the accuracy of predicting peak GRFz from duty factor (the proportion of the stride for which the limb is in contact with the ground). Foot-mounted uniaxial accelerometers, combined with UHF FM telemetry, are shown to be practical and accurate for the field measurement of stride timing variables, including duty factor. Direct comparison with the force plate produces a mean error of 2.3 ms and 3.5 ms for the timing of foot on and foot off, respectively, across all gaits. Predictions of peak GRFz from duty factor show mean errors (with positive values indicating an overestimate) of 0.8±0.04 N kg$^{-1}$ (13%; *N*=42; mean ± S.E.M.) at walk, –0.3±0.06 N kg$^{-1}$ (3%; *N*=75) at trot, –2.3±0.27 N kg$^{-1}$ (16%; *N*=18) for the non-lead limb at canter and +2.1±0.7 N kg$^{-1}$ (19%; *N*=9) for the lead limb at canter. The substantial over- and underestimate seen at canter, in the lead and non-lead limbs, respectively, is attributed to the different functions performed by the two limbs in the asymmetrical gaits. The difference in load experienced by the lead and non-lead limbs decreased with increasing speed.**

Key words: ground reaction force, field locomotion, accelerometer, duty factor, horse.

## Introduction

The maximum vertical ground reaction force (peak GRFz) experienced by an individual limb during ground contact has been shown to constrain maximum running speed in humans and has been proposed as a trigger for gait transition in both bipeds and quadrupeds (Weyand et al., 2001; Farley and Taylor, 1991; Hreljac, 1993; Nilsson and Thorstensson, 1989; Wickler et al., 2003). Limb force also determines the load experienced by musculoskeletal structures, the safety factors involved in high-speed locomotion and the cost of locomotion (Biewener, 1990; Kram and Taylor, 1990). Peak GRFz also determines the risk of fractures and other musculoskeletal injuries in horses and has been used in the assessment of lameness (Merkens and Schamhardt, 1988a,b). In addition, the magnitude and time course of forces experienced by the limbs are important in eliciting a positive, or negative, bone remodelling response.

Force is routinely measured with high precision and accuracy in the laboratory environment using a force plate (Elftman, 1938; Cavagna et al., 1964; Pratt and O'Connor, 1976). Force plates, however, have a number of drawbacks. They are expensive, need to be mounted in a purpose-built runway and rely on the subject hitting the plate with exactly one leg. More recently, force platforms have been incorporated into treadmills, offering advantages over standard installations, but studies are still limited to the laboratory environment.

We are particularly interested in the horse (*Equus caballus*) as a model system for the study of locomotion. The horse has evolved a highly specialised musculoskeletal system and is capable of short bursts of high-speed locomotion as well as more sustained exercise at lower speeds.

Pressure-sensitive insoles are commonly used in human biomechanics; however, their application in horses is limited as the technology is expensive and fragile, and absolute calibration values are poor (Hennig et al., 1982; Cavanagh et al., 1983). A number of groups have developed instrumented horseshoes and have achieved increasing levels of accuracy (Marey, 1882; Björk, 1958; Frederick and Henderson, 1970; Hügelshofer, 1982; Kai et al., 2000; Ratzlaff et al., 1985, 1990; Roepstorff and Drevemo, 1993). However, it is still difficult to record the entire force transmitted by the foot while maintaining the requirements for grip, all in a thin construct of minimal mass. Even small changes in digital mass may have significant effects on kinematics due to the rapid accelerations experienced during the gait cycle (Back et al., 1995).

Limb force has been predicted from kinematic data, although this is difficult. We have demonstrated that, in horses,

there is a gait-independent linear relationship ($r^2$=0.95–0.99) between the peak extension angle (the posterior angle subtended by the axis of the third metacarpal bone and the axis of the phalanges) of the metacarpophalangeal (MCP) joint and limb force (McGuigan and Wilson, 2003). The joint angle–force relationship can be calibrated at low speed using a force plate, and subsequently limb force can be predicted from kinematics at higher speeds. The method is, however, limited to the horse and requires the collection of kinematic data, which is difficult outdoors.

Cine film has been used to estimate limb force in galloping buffalo (*Syncerus caffer*) and ambling elephant (*Loxodonta africana*) by applying the principle of conservation of momentum (Alexander et al., 1979). In steady-state locomotion, the total vertical impulse (the integral of force with respect to time) applied to the centre of mass during a stride must equal the product of body weight and the stride duration. There is, therefore, an inverse relationship between stance time and peak vertical force if a limb generates a certain impulse. That fraction of the stride time for which the limb transmits force to the ground (i.e. the limb is in the stance phase) is known as the duty factor. Alexander and co-workers used these concepts, and the observation that the GRF–time curve in a spring-like or running gait is approximately sinusoidal in shape, to generate the following equation:

$$Fz_{max} = \pi pmg/4\beta \ , \quad (1)$$

where $Fz_{max}$ is peak vertical ground reaction force (N), $p$ is the proportion of the mass of the animal carried by the pair of legs in question (conventionally 0.6 and 0.4 for the front and rear pairs, respectively), $m$ is the mass of the animal (kg), $\boldsymbol{g}$ is the gravitational constant (9.81 m $s^{-2}$) and $\beta$ is the duty factor.

The accuracy of this calculation relies on three assumptions and/or constants:

(1) The shape of the GRF curve. In biology, the shape of the GRF curve is not the result of a simple oscillating spring–mass system. Geometric compression of the leg spring due to forward motion of the trunk over the planted foot and anatomical design causes the resultant curve to differ from a pure sine wave (Farley et al., 1993). This shape effect has been demonstrated in kangaroos (*Macropus rufus*), where it resulted in a 36% underestimation of GRFz predicted using equation 1 (Kram and Dawson, 1998). The shape of the GRF curve in the horse, where there is an apparently simpler lever system, has not been compared to a pure sine wave.

(2) The proportion of the body mass supported by the front and hind legs. This is traditionally stated to be 60% or more on the forelimbs (Hoyt et al., 2000). The exact origin of this figure is hard to trace (Stashak, 2002); however, the figure can be derived for other quadrupeds from the data of Cavagna et al. (1977) and others. In our momentum-based calculation, the proportion assigned should relate to the relative impulse generated by the front and hind legs rather than simply the peak limb force.

(3) The symmetry of limb GRF curves between pairs of legs in asymmetrical gaits. Bipedal skipping and quadrupedal canter and gallop are termed asymmetrical gaits because the foot strikes of contra-lateral limbs are not evenly spaced in time (Gambaryan, 1974; Hildebrand, 1989). In contrast to human bipedal skipping, where peak limb force has been shown to be the same in both limbs of the pair (Minetti, 1998), the limbs of a horse performing an asymmetrical gait experience markedly different peak GRFz (Biewener et al., 1983; Merkens et al., 1993; McGuigan and Wilson, 2003). The first limb to contact the ground after the aerial phase is known as the non-lead leg, and the limb that leads into the aerial phase is known as the lead leg. The non-lead limb experiences a 25% greater peak force than the lead limb at slow canter (Merkens et al., 1993), and a similar difference has been predicted at higher speeds (McGuigan and Wilson, 2003). However, the stance duration and duty factor are very similar between the lead and non-lead limb (Back et al., 1997). In fact, using the data of Back et al. (1997), equation 1 would predict only a 3% difference in limb force between the forelimbs. It therefore appears that an offset or correction factor is required in order to give an accurate prediction of limb force from duty factor at asymmetrical gaits.

Application of the above technique for the prediction of peak GRFz requires that stance time be accurately determined. Direct GRF measurement, accelerometer data and kinematic methods have been compared for the objective determination of the timing of foot on and foot off (Schamhardt and Merkens, 1994). Force plate data are extremely accurate for both initial ground contact time and the time of foot off. Kinematic analysis alone, on the other hand, was reported to be insufficiently accurate for the determination of either parameter. Analysis of digital acceleration offers an alternative and has been used to develop a tool for the estimation of aerobic power during walking and running in humans (Weyand et al., 2001). This method, however, also has potential disadvantages. In the late stance phase, the foot pivots about the toe (an event known as heel off) prior to the foot completely leaving the ground (Fig. 1; Schamhardt and Merkens, 1994). The error in stance time determination was 14.6% in a study of humans, which was attributed to the inability to differentiate foot rotation from actual foot off (Weyand et al., 2001). We propose that, in the horse, toe off can be accurately detected and differentiated from heel off using an appropriately mounted accelerometer due to the changes in the direction of foot acceleration.

The ability to accurately determine the vertical force experienced by all four limbs of large cursorial animals during high-speed locomotion in the field would contribute greatly to our understanding of the athletic ability of these animals, since peak limb force has been identified as limiting to running speed. In order to apply the technique described by Alexander et al. (1979), we must first validate a method for determining the stride timing variables used to calculate duty factor. Subsequently, the assumptions that equation 1 relies on must be validated. It would therefore be useful to compare the actual GRF curves to a sine wave of the same base and area and to determine whether this method provides a good estimate of GRF throughout the stride or only at the peak value.

The goal of this study was first to evaluate the accuracy of a system of limb-mounted accelerometers for detecting foot on and foot off in the horse. Second, foot on and foot off data would be used to test the hypothesis that peak GRFz can be predicted from duty factor. Specifically, experiments were designed to answer the following questions: (1) can the timing of foot on and foot off be determined using data from foot-mounted accelerometers during locomotion on both hard and soft surfaces; (2) what is the ratio of front–hind impulses as a function of speed and gait and (3) can the approach of Alexander et al. (equation 1) be applied to walking and asymmetrical gaits?

## Materials and methods

Two experiments were performed. First, the timings of foot on and foot off events were determined simultaneously by force plate and accelerometry during led walk, trot and canter. Peak limb force was determined by force plate measurement and calculated from duty factor using equation 1. Second, maximum MCP joint extension angle was measured for the lead and non-lead forelimbs during high-speed treadmill locomotion in order to quantify peak limb force asymmetry at higher speeds.

### *Determination of foot on and foot off and peak limb force at walk, trot and canter on a hard surface*

Six Warmblood-type riding horses (mass 573–705 kg; mean 636 kg) were used for the walk and trot experiment, and four fit Thoroughbred horses (mass 453–512 kg; mean 488 kg) were used for the cantering. All subjects were assessed as being free of lameness by veterinary examination prior to each experiment. Foot acceleration was measured using solid-state capacitive accelerometers with a dynamic range of ±50 g (ADXL150, Analog Devices, Norwood, MA, USA; sensitivity 38 mV $g^{-1}$). These were protected by enclosure in epoxy-impregnated Kevlar fibres (total mass 2 g) and mounted on the dorsal midline of the hoof, with the sensitive axis orientated in a proximo-distal direction, using hot melt glue from a hot glue gun (Bostik Findley Inc., Stafford, UK). The optimum position and range of the accelerometer was first determined by experimentation with both ±5 g and ±50 g accelerometers and with mounting on the lateral aspect of the third metacarpal/metatarsal bone (MC/MT), the lateral and dorsal aspects of the proximal phalanx and various positions on the foot during locomotion on both hard and soft surfaces. Output signals were telemetered *via* programmable narrow-band analogue FM radio telemetry devices operating at 458 MHz (ST/SR500; Wood and Douglas Ltd, Tadley, Hampshire, UK) and logged *via* a 12-bit A/D converter and PCMCIA card (DAQcard700; National Instruments, Newbury, Berkshire, UK) into a laptop computer running custom software in LabView (National Instruments). The telemetry transmitter, ¼ wave whip antenna and NiCad battery were mounted in a custom-designed exercise bandage on the lateral aspect of the MC/MT (mass of telemetry unit 73 g and battery 88 g; total mass of bandage with telemetry unit, 376 g). A short, fatigue-resistant cable was constructed of multi-strand copper wire coiled around a flexible 2 mm-diameter core of mountaineering cord and coated in silicon rubber (Wilson and Goodship, 1994). This highly flexible cable ran along the lateral aspect of the digit and linked the telemetry unit to the accelerometer (Fig. 2).

Horses were led by an experienced handler along an 80-m dirt and concrete runway in which a force plate was embedded

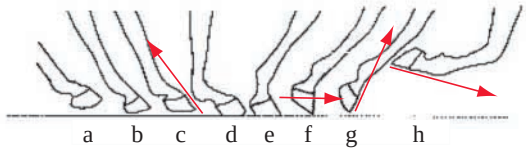


Fig. 1. The orientation of the equine digit during foot on and foot off. The accelerometer is mounted axially on the dorsal hoof wall with the sensitive axis orientated disto-proximally. Critically, the foot acceleration vector (indicated by the red arrows) is orientated along the sensitive axis of the accelerometer at foot on (d) and at foot off (g). However, during roll over (f), when the heel of the foot (the most rearward point of the ground-bearing surface) has left the ground and the foot is rotating around the toe (the most forward point of the ground-bearing surface), the vector is orientated orthogonal to the sensitive axis.

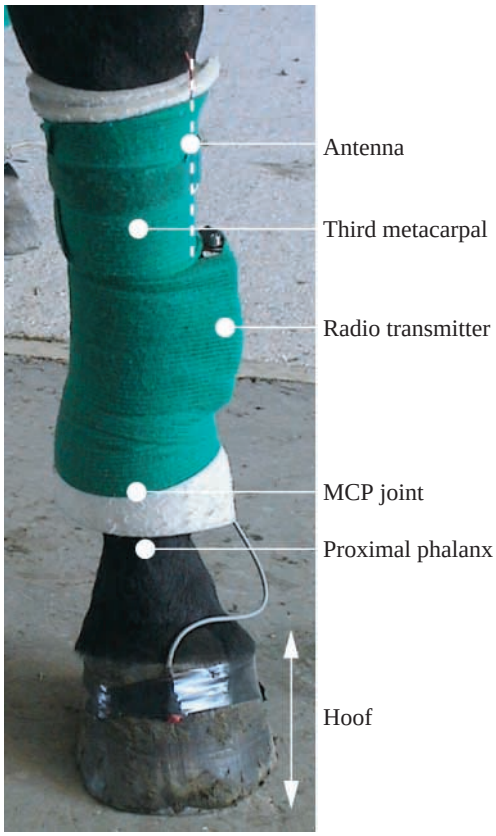


Fig. 2. An accelerometer and telemetry unit in place on the distal limb of a horse. The telemetry unit and battery are contained within the exercise bandage and mounted on the lateral aspect of the third metacarpal bone. The accelerometer is encased in epoxy and Kevlar fibres, mounted on the dorsal surface of the hoof and protected from abrasion by the exercise surface with electrical insulation tape.

(Kistler 9287BA; Kistler Instruments Ltd, Alton, Hampshire, UK). Both force plate and runway were covered in commercial conveyor belt matting. Force data were amplified by integral charge amplifiers, filtered through a low-pass filter (6 dB octave$^{-1}$ from 50 Hz) and collected simultaneously with accelerometer data in LabView (National Instruments). All data were logged at 1000 Hz.

The time of foot placement (foot on) was taken as the first frame in which the vertical force rose above 50 N, and foot off was defined as being the first frame in which the vertical force (GRFz) fell below 50 N (Clayton et al., 1999). In the horse, the well-defined increase and decrease in GRFz, which occur at foot on and foot off, respectively, mean that a 50 N threshold accurately identified the timing of these events. These times were used to visually assess the accelerometer data and define the acceleration features that corresponded to foot on and foot off. The operator was then blinded to the force data for the remainder of the analysis. The times of foot on and foot off were manually extracted from the accelerometer traces using transcription freeware (http://www.etca.fr/CTA/gip/Projets/Transcriber). For each stride, the times of foot on and foot off, as determined using the force plate, were subtracted from those determined using the accelerometer such that an error value was obtained that was negative if the accelerometer time was early and positive if it was late. From the accelerometer data, total stride period was defined as the difference between two sequential foot on events, and stance period as the time between foot on and the subsequent foot off. Duty factor was then calculated as the ratio of stance period to stride period and was used to calculate $Fz_{max}$ using equation 1. Force plate data were used to calculate ratios of front to hind peak vertical force and front to hind vertical impulse, although for canter data this was only possible for non-lead limbs. Peak vertical force was determined for each limb strike and compared with the predicted force.

*Measurement of MCP joint angle during high-speed treadmill locomotion*

Flat, circular retro-reflective markers (Scotchlite 8850; 3M, Bracknell, Berkshire, UK), 20 mm in diameter, were placed at the following skeletal landmarks on the lateral aspect of the left forelimbs and the medial aspect of the right forelimbs of the same four Thoroughbred horses used in experiment 1: (1) proximal end of the fourth metacarpal; (2) proximal attachment of the lateral/medial collateral ligament of the MCP joint to the distal third metacarpal bone (centre of rotation of the MCP joint) and (3) lateral/medial hoof wall approximately over the centre of rotation of the distal inter-phalangeal (DIP) joint.

The horses had been habituated to locomotion on a high-speed treadmill (Satö, Knivsta, Sweden; Buchner et al., 1994). During the experiment, they wore neoprene brushing boots and over-reach boots to avoid interference injuries while galloping. After a warm-up period, the horses were exercised at increments of speed between 1.6 m s$^{-1}$ and 12 m s$^{-1}$. During canter locomotion it was recorded whether the left forelimb or the right forelimb was the lead leg. Marker location in the sagittal plane was recorded from the horses' left side (ProReflex; Qualisys AB, Gothenburg, Sweden). At each speed increment, the horse was allowed 20 s to settle into a steady gait pattern prior to the collection of 10 s of data.

MCP joint extension angle was calculated as the posterior angle subtended by the axes of the third metacarpal bone and proximal phalanx. The peak angle was determined for each stride of each file, and the mean peak MCP angle was determined for both front legs at each speed increment.

## Results

The features attributed to foot on and foot off are presented along with the corresponding vertical force traces in Fig. 3. A high-frequency, high-amplitude acceleration signal was seen at

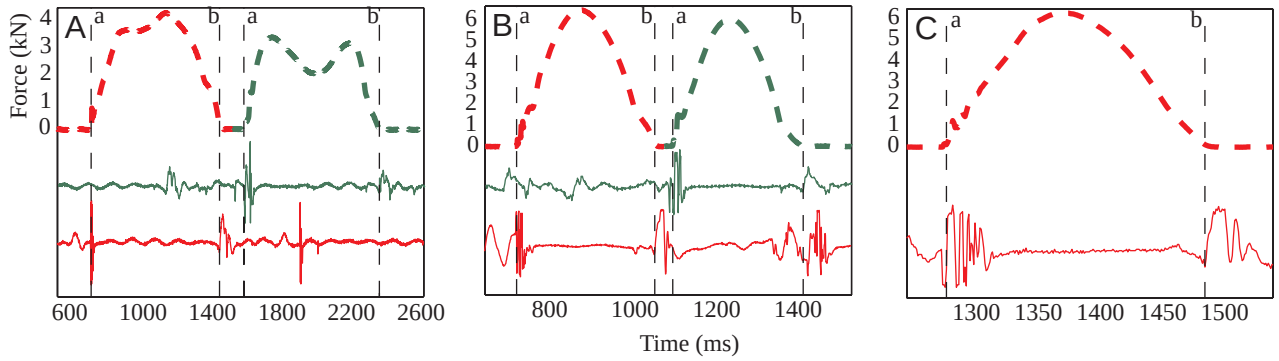


Fig. 3. Representative graphs of simultaneous peak vertical ground reaction force (GRFz) and accelerometer data collected during walk (A), trot (B) and canter (C) locomotion. For walk and trot trials, force plate data were collected for both front limbs (red broken line) and hind limbs (green broken line) during the same trial. Beneath the force outputs, the corresponding accelerometer traces are shown. Vertical broken lines indicate the timing of foot on (a) and foot off (b). The red solid line indicates the output from the forelimb accelerometer, and the green solid line the hind limb accelerometer data. Note the precipitous rise in force at foot on and the rapid drop in force at foot off, which allow the accurate determination of foot on and foot off from vertical force data alone. Also note the absence of features in the accelerometer trace during the stance phases, except a minor undulation shortly prior to foot off, corresponding to heel off and foot rotation. The automatic gain control in the telemetry link means that whilst the accelerometer signal amplitude is the same in all three plots, the actual acceleration will differ.

the time of foot on. This was followed by a short burst of high frequency oscillations and then a plateau while the foot was in stance. Subsequently, a lower frequency peak was seen to coincide with foot off, a feature that was easily distinguishable from the heel lift and foot rotation that occurred prior to foot off. Heel lift and foot rotation were prominent if the accelerometer was mounted on the proximal phalanx, especially on a soft surface, but were only evident as a very minor low-frequency oscillation with hoof mounting (see Fig. 4). These features were consistent on both hard and soft surfaces, across the gaits and between individuals.

The features were most obvious and distinctive when the accelerometer was positioned on the dorsal hoof wall, orientated with the sensitive axis along the midline of the limb (Fig. 4). Initial experiments with the accelerometer mounted on the lateral aspect of the proximal phalanx resulted in satisfactory acceleration features corresponding to the foot on event; however, foot off became difficult to detect reliably, especially on a soft surface.

In the first experiment, a total of 147 stance phases were collected (46 at walk, 75 at trot and 26 at canter). Mean absolute error for foot on time was 2.4 ms at walk (median error –2 ms, inter-quartile range –2 to –1 ms), 1.8 ms at trot (median –1 ms, IQR –2 to +1 ms), 2.0 ms (median 1.5 ms, IQR +1 to +2 ms) for the non-lead limb and 3.0 ms (median 2.5 ms, IQR +1.5 to +3 ms) for the lead limb at canter. Mean absolute error for foot off time was 3.6 ms at walk (median –2 ms, IQR –5 to +1 ms), 2.4 ms at trot (median –1 ms, IQR –4 to 0 ms), 5.0 ms for the non-lead limb (median –4 ms, IQR –10 to +9 ms) and 2.8 ms for the lead limb (median –2 ms, IQR –7 to –1 ms) at canter.

In order to test the validity of the assumption that GRFz follows a sinusoidal curve as required by equation 1, we superimposed sine waves of the same base and area on each GRFz curve generated in experiment one. The amplitude of the sine wave generated was subtracted from the peak GRFz measured in each case. This produced an error value, which was positive if the peak GRFz was overestimated and negative if it was underestimated. Fig. 5 shows mean (± S.D.) GRFz curves across all strides recorded for front and hind limbs at walk and trot and lead and non-lead forelimbs at canter. The superimposed sine waves lie within 1 S.D. of the mean force for between 40% and 70% of the stride for both front and hind limbs at trot and canter. The mean value of the amplitude error was 0.3 N $kg^{-1}$ (4% of peak GRFz; $N$=72; range –1.1 to +1.3 N $kg^{-1}$) at walk, –0.8 N $kg^{-1}$ (7% of peak GRFz; $N$=109; range –2.1 to 0.7 N $kg^{-1}$) at trot, –0.6 N $kg^{-1}$ (5% of peak GRFz; $N$=36; range –1.1 to 0.3 N $kg^{-1}$) for the non-lead limb at canter and –0.4 N $kg^{-1}$ (3% of peak GRFz; $N$=7; range –0.6 to –0.2 N $kg^{-1}$) for the lead limb at canter (Fig. 6).

The ratios of front to hind peak vertical force and front to hind vertical impulse were calculated and are expressed as percentages and plotted against peak GRFz for all strides in Fig. 7. Linear regression of front:hind force ratio against absolute forelimb force showed that the force ratio was gait dependent ($y$=1.6198–0.0358$x$, $r^2$=0.272, $P$<0.0001). The

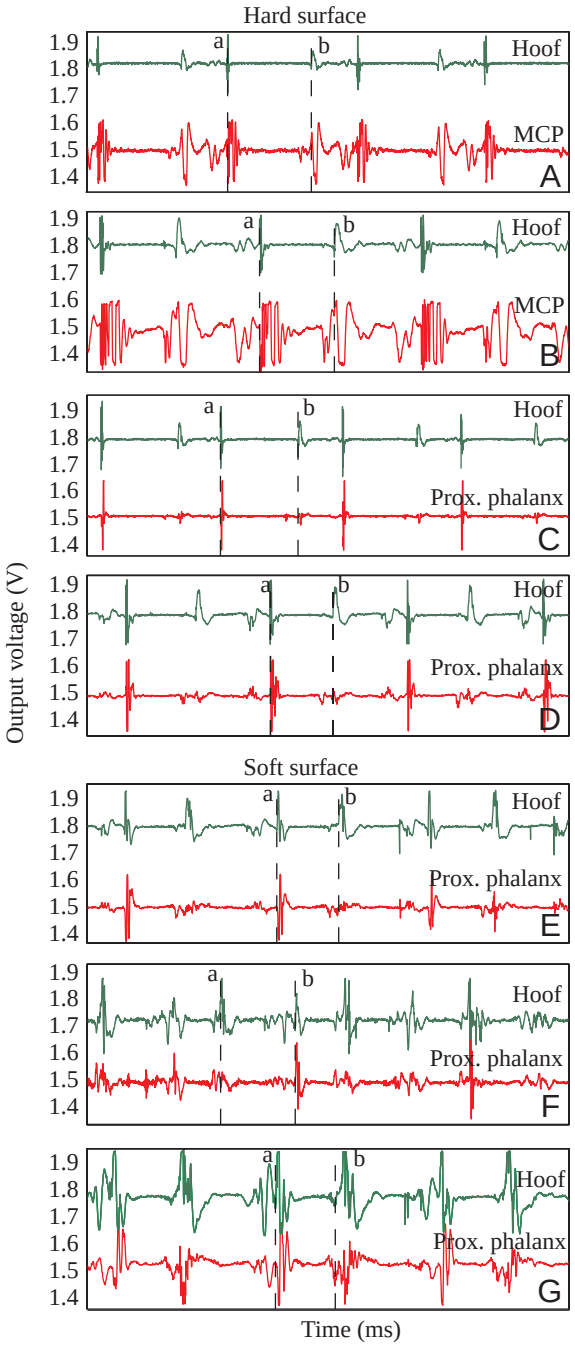


Fig. 4. Comparison of different accelerometer mounting positions by simultaneous collection of data from several accelerometer locations. The output for the hoof-mounted accelerometer is always shown in green, and the comparison location in red. The output during locomotion on a hard surface of an accelerometer mounted on the lateral aspect of the third metacarpal bone (MCP) at walk (A) and trot (B), and the output of an accelerometer mounted on the proximal phalanx (prox. phalanx) during walk (C) and trot (D) are shown. The output during soft surface locomotion of an accelerometer mounted on the proximal phalanx during walk (E), trot (F) and canter (G) is also shown. Vertical broken lines indicate the time of foot on (a) and foot off (b). Accelerometer output in volts cannot be converted to m $s^{-2}$ due to automatic gain control within the analogue telemetry system used.

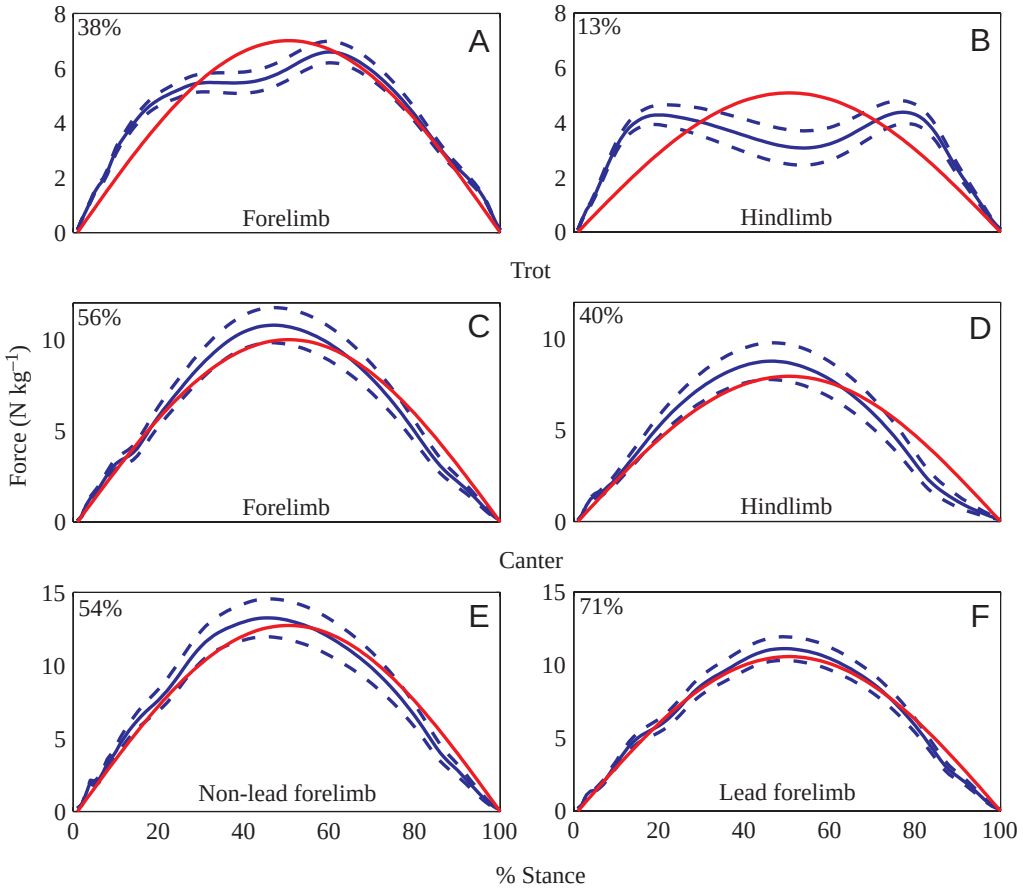


Fig. 5. Mean (± S.D.; broken lines) vertical ground reaction force (blue) relative to percentage of stance duration for the forelimb and hind limb at walk (A,B) and trot (C,D), and lead and non-lead forelimbs at canter (E,F). A sine wave of equal base and area is superimposed in red over the ground reaction force. Values in the upper left corner of each graph indicate the percentage of the stance time for which the sine wave lies within 1 S.D. of the mean force.

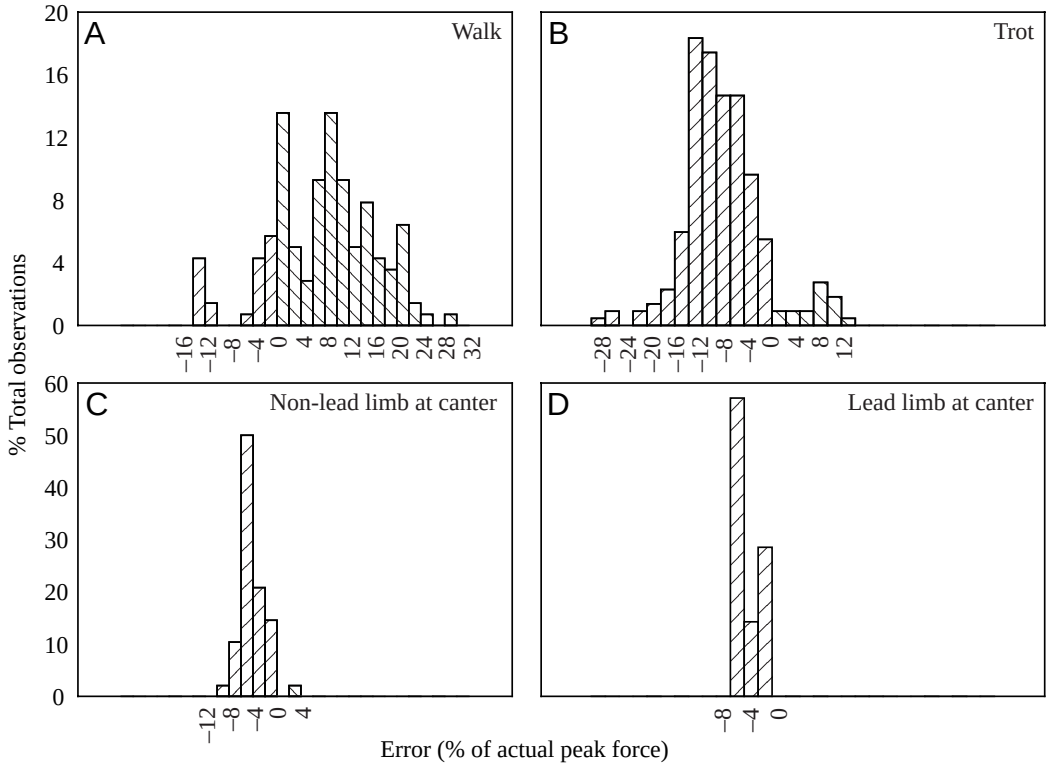


Fig. 6. Histograms showing the distribution of errors in peak limb force prediction for individual stance phases using a sine wave of same base and area at walk (A) and trot (B) and for the non-lead (C) and lead limbs (D) at canter.

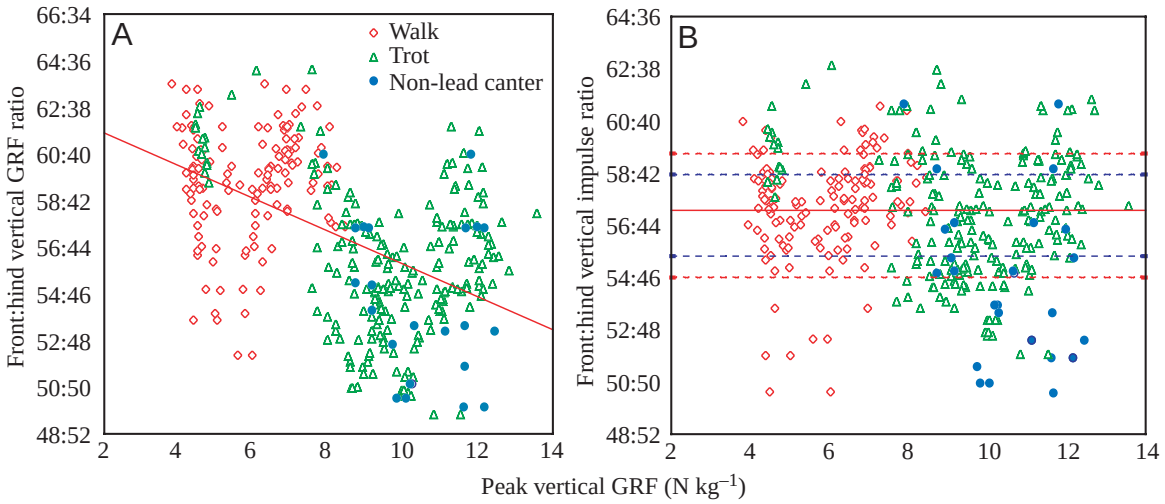


Fig. 7. (A) Plot of front:hind ratio of peak vertical ground reaction force (GRFz) *versus* peak forelimb GRFz, expressed as percentages. Data are shown for walk (red diamonds), trot (green triangles) and canter non-lead leg (filled blue circles). The linear regression line is fitted to all data ($y$=1.6198–0.0358$x$, $r^2$=0.2722, $P$<0.0000). (B) Plot of front:hind vertical impulse ratio *versus* peak GRFz, expressed as percentages. Symbols are as for A. The horizontal red solid line shows the mean ratio across all speeds (1.33). The red broken lines indicate ± S.D., and the blue broken lines indicate the inter-quartile range.

mean front:hind force ratio (± S.D.) was 1.44±0.12 ($N$=140) at walk, 1.32±0.49 ($N$=218) at trot and 1.18±0.17 ($N$=23) for the non-lead limbs at canter. The ratio of vertical impulse, however, was minimally affected by speed and gait ($y$=1.3724–0.0064$x$, $r^2$=0.018, $P$=0.0081). The average front:hind vertical impulse ratio was 1.33±0.11 (mean ± S.D.). This equates to a percentage vertical impulse distribution (front:hind) of 57%:43%. This impulse distribution was used in the subsequent calculations of predicted peak GRFz from duty factor.

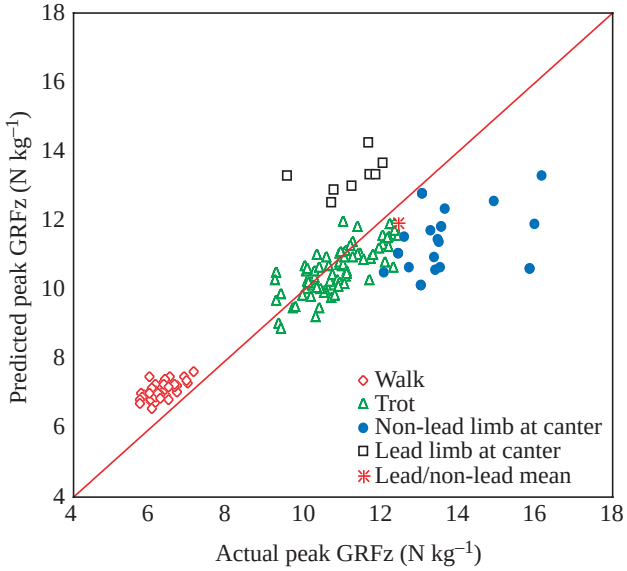


Fig. 8. Scatter plot of predicted peak vertical ground reaction force (GRFz) *versus* actual peak GRFz. Both are normalised to body mass. Data are shown for walk (red diamonds), trot (green triangles), non-lead leg at canter (blue circles) and lead leg at canter (black squares). The red line indicates the function $y$=$x$. The red star shows the position of the mean of the average lead and non-lead limb data.

A scatter plot of predicted peak GRFz *versus* actual peak GRFz for all strides is shown in Fig. 8. This shows that the prediction is a slight overestimate for all walk strides, good for all trot strides but underestimates the non-lead leg peak force and overestimates the lead leg peak force at canter. Error was negative if the prediction underestimated the actual value. The mean error was 0.8 N kg$^{-1}$ (13% of peak GRFz; range 0.3–1.5 N kg$^{-1}$) at walk, –0.3 N kg$^{-1}$ (3% of peak GRFz; range –1.7 to 1.2 N kg$^{-1}$) at trot, –2.3 N kg$^{-1}$ (17% of peak GRFz; range –5.2 to –0.3 N kg$^{-1}$) for the non-lead limb at canter and 2.1 N kg$^{-1}$ (19% of peak GRFz; range 1.5–3.7 N kg$^{-1}$) for the lead limb at canter. When the means of the lead and non-lead limbs are plotted on the same graph, the point is very close to the line of normality.

Fig. 9 shows the difference in peak MCP joint angle between the forelimbs plotted against speed for four horses. Because absolute angle values could differ due to differences in marker placement between the left and right limbs, the data have been normalised to ensure symmetry at a trot speed of 3 m s$^{-1}$. At canter, the mean difference in peak MCP angle between the two limbs decreased by a factor of three from 7.0° at the lowest speed (7 m s$^{-1}$) to 2.4° at the highest speed examined (12 m s$^{-1}$).

## Discussion

Determination of the timing of foot off with accelerometers is difficult. Previous studies have mounted the accelerometer perpendicular with the ground surface, whereas here we mounted it along the dorsal hoof wall with the sensitive axis parallel to the long axis of the limb (Fig. 2; Schamhardt and Merkens, 1994). This means that during foot rotation prior to

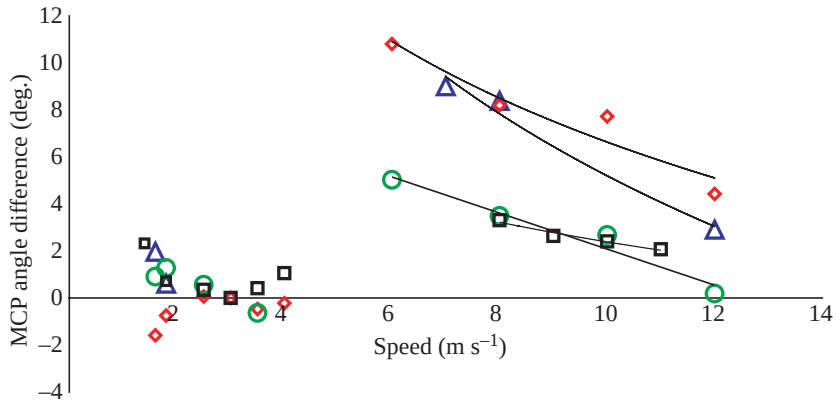


Fig. 9. Difference in metacarpophalangeal (MCP) joint extension angle between left and right forelimbs during treadmill locomotion at a range of speeds and gaits for four horses. Colours indicate individual horses.

foot off, no component of the acceleration is transduced (Fig. 1). At foot off, however, the acceleration vector is aligned with the long axis of the limb, and hence the sensitive axis of the accelerometer, and the majority of the acceleration is detected. Hoof mounting therefore provided clear and repeatable features during both hard surface and soft surface locomotion at all gaits and represented the optimum site of accelerometer placement, although this location is less convenient than higher up the leg. Due to its low mass and small size, attachment of the accelerometer to the dorsal hoof wall was straightforward and rarely failed. The Kevlar and epoxy casing ensured that the electronic components remained safe even when the attachment failed. The connecting cable was found to be the weakest point, prompting the design of a strong, fatigue-resistant, yet highly flexible cable.

The mass of the equine metacarpus and digit is 3420 g (Buchner et al., 1997). Horses commonly wear brushing boots (mass 200–400 g) to prevent injury from interference between limbs during training and racing. The combined mass of the accelerometer, telemetry unit, battery and exercise bandage (376 g) is within the mass range of commercial brushing boots and is therefore unlikely to interfere with normal kinematics. In one study, attaching 88 g weights to the toes of Standardbred trotters had minimal effect on stride length, stride duration and the relative duration of stance and swing phases as a percentage of the stride (Willemen et al., 1994). Our equipment is mounted further proximal on the limb, where the effect on kinematics will be even less. In addition, the equipment could be made lighter by reducing the battery size (currently 88 g) or by using a smaller, and lower power, telemetry transmitter.

The four-limb telemetry system presented some technical difficulties during design. The effect of four transmitters in close proximity to one another and the reradiating and/or shielding effect of the horse was expected to significantly reduce the range from the manufacturers' claimed line of sight ranges of up to 2 km. However, during the series of experiments described here, undertaken at ranges of up to 300 m, signal reception and strength was never a problem. Analogue telemetry links use automatic gain control to ensure that the dynamic range of the system is used. The output voltage is therefore proportional to acceleration through the stride, but actual acceleration values cannot be obtained. This is seen in Figs 3, 4, where input amplitude will vary but the output amplitude remains the same.

Equation 1 relies on the sinusoidal nature of the GRFz–time curve. This assumption holds true for the running gaits, where the limb compresses and extends during the stance phase to store and return elastic energy. In comparison, walking gaits are traditionally modelled as an inverted pendulum with the trunk vaulting over a relatively incompressible limb, resulting in a bimodal GRF–time curve. It is interesting, therefore, that the technique presented still provides a reasonable estimate of limb force at walk. Indeed, the predictions for walking are more accurate than those for slow cantering (Fig. 8). In the horse, walking still has spring-like properties although with less leg compression and reduced trunk lift at mid-stance.

During trot locomotion, the prediction of force from duty factor was shown to be accurate. However, during canter locomotion, equation 1 provided an underestimate for the non-lead limb and an overestimate for the lead limb. A considerable asymmetry therefore exists in the impulse applied by the two forelimbs since sine wave assumption was similar (Figs 5, 6).

Equation 1 requires knowledge of the distribution of the mass of the animal between the front and hind limbs. This should consider the ratio of the vertical impulses rather than simply the peak force since the equation is based upon momentum. This study shows that although the front:hind impulse distribution and the front:hind force distribution are both similar at 57:43, the front:hind peak force ratio did decrease with gait from walk to trot and canter. The reason for this change is unknown. The impulse distribution was shown not to change within the speed range studied and it is therefore appropriate to use the same ratio for all gaits in the calculation of peak force.

During this study, horses were examined on a treadmill at a range of canter speeds. As speed increased, the difference in MCP joint extension angle (linearly related to vertical limb force) between the lead and non-lead legs decreased. Using the previously published population regression of limb force against MCP joint angle of McGuigan and Wilson (2003), this equates to a reduction in lead–non-lead force difference from 1.8 N $kg^{-1}$ to 0.5 N $kg^{-1}$. This indicates that as speed increases, limb function becomes more symmetrical. At maximum racehorse running speed (18 m $s^{-1}$), therefore, the error in peak

GRFz prediction may be greatly reduced. On the scatter plot of predicted *versus* actual force, the mean of lead and non-lead limbs lies very close to the line of normality (Fig. 8). This confirms that the GRFz trace is inherently sinusoidal in nature and that the non-lead leg simply generates a larger impulse. It also suggests that the distinct tail of the canter GRFz trace (Fig. 5) does not contribute to prediction inaccuracy. It may be possible to generate a speed-dependent correction factor to increase the accuracy of the force prediction during asymmetrical gaits; however, the lead–non-lead difference in absolute peak limb force is variable between individuals (Fig. 9). The reduction in peak angle asymmetry seen at higher speeds suggests that such a correction may be unnecessary for studies of maximum speed locomotion. The peak angle asymmetry seen here at high speed is generally less than we found previously (7.7°), where only one leg per horse was analysed (McGuigan and Wilson, 2003).

The superimposed sine wave of the same base and area did have a similar shape to the GRFz curve at both trot and canter. This demonstrated that the method can also be used to estimate GRFz with reasonable accuracy throughout stance at these gaits and not just at mid stance.

The system of limb-mounted accelerometers described in this paper proved to be practical for use in field conditions, making it possible to estimate the mechanical environment of the skeleton in individual horses and consider the factors that limit gallop speed in horses under different environmental conditions. In the future, it may be possible to automate the detection of the features in the accelerometer output in order to reduce the time required for data analysis.

### *Conclusions*

It is possible to accurately predict peak GRFz from duty factor in the horse. For asymmetrical gaits, a correction factor is required to compensate for the difference between the lead and non-lead limbs of a pair. Mean peak limb force can, however, be accurately determined for asymmetrical gaits. The system described offers the potential for studying peak forces and bone and tendon loading during field exercise.

The authors would like to acknowledge the Horserace Betting Levy Board for funding the work of T.H.W. and the BBSRC for providing additional funding. The Household Cavalry Mounted Regiment is acknowledged for providing horses and handlers. Polly McGuigan, Rachel Payne, Glen Lichtwark and Jo Watson are thanked for assistance with data collection.

## References

**Alexander, R. McN., Maloiy, G. M. O., Hunter, B., Jayes, A. S. and Nturibi, J.** (1979). Mechanical stresses during fast locomotion of buffalo (*Syncerus caffer*) and elephant (*Loxodonta africana*). *J. Zool. Lond.* **189**, 135-144.

**Back, W., Schamhardt, H. C., Hartman, W. and Barneveld, A.** (1995). Kinematic differences between the distal portions of the forelimbs and hind limbs of horses at the trot. *Am. J. Vet. Res.* **56**, 1522-1528.

**Back, W., Schamhardt, H. C. and Barneveld, A.** (1997). Kinematic comparison of the leading and trailing fore- and hindlimbs at the canter. *Equine Vet. J. Suppl.* **23,** 80-83.

**Biewener, A. A.** (1990). Biomechanics of mammalian terrestrial locomotion. *Science* **250**, 1097-1103.

**Biewener, A. A., Thomason, J., Goodship, A. and Lanyon, L. E.** (1983). Bone stress in the horse forelimb during locomotion at different gaits: a comparison of two experimental methods. *J. Biomech.* **16**, 565-576.

**Björk, G.** (1958). Studies on the draught forces of horses: development of a method using strain gauges for measuring forces between hoof and ground. *Acta. Agric. Scand* **8**, Suppl. 4.

**Buchner, H. H., Savelberg, H. H., Schamhardt, H., Merkens, H. W. and Barneveld, A.** (1994). Habituation of horses to treadmill locomotion. *Equine Vet. J. Suppl.* **17**, 13-15.

**Buchner, H. H., Savelberg, H. H., Schamhardt, H. C. and Barneveld, A.** (1997). Inertial properties of Dutch Warmblood horses. *J. Biomech.* **30**, 653-658.

**Cavagna, G. A., Saibene, F. P. and Margaria, R.** (1964). Mechanical work in running. *J. Appl. Physiol.* **19**, 249-256.

**Cavagna, G. A., Heglund, N. C. and Taylor, C. R.** (1977). Mechanical work in terrestrial locomotion: two basic mechanisms for minimizing energy expenditure. *Am. J. Physiol.* **233**, R243-R261.

**Cavanagh, P. R., Hennig, E. M., Bunch, R. P. and Macmillan, N. H.** (1983). A new device for the measurement of pressure distribution inside the shoe. *Biomechanics* **III-B**, 1089-1096.

**Clayton, H. M., Lanovaz, J. L., Schamhardt, H. C. and van Wessum, R.** (1999). The effects of a rider's mass on ground reaction forces and fetlock kinematics at the trot. *Equine Vet. J. Suppl.* **30**, 218-221.

**Elftman, H.** (1938). The measurement of the external forces in walking. *Science* **88**, 152.

**Farley, C. T. and Taylor, C. R.** (1991). A mechanical trigger for the trot–gallop transition in horses. *Science* **253**, 306-308.

**Farley, C. T., Glasheen, J. and McMahon, T. A.** (1993). Running springs: speed and animal size. *J. Exp. Biol.* **185**, 71-86.

**Frederick, F. H., Jr and Henderson, J. M.** (1970). Impact force measurement using preloaded transducers. *Am. J. Vet. Res.* **31**, 2279-2283.

**Gambaryan, P. P.** (1974). Gaits of mammals. In *How Mammals Run: Anatomical Adaptations*, pp. 14-62. New York: John Wiley & Sons.

**Hennig, E. M., Cavanagh, P. R., Albert, H. T. and Macmillan, N. H.** (1982). A piezoelectric method of measuring the vertical contact stress beneath the human foot. *J. Biomed. Eng.* **4**, 213-222.

**Hildebrand, M.** (1989). The quadrupedal gaits of vertebrates. *BioScience* **39**, 766-775.

**Hoyt, D. F., Wickler, S. J. and Cogger, E. A.** (2000). Time of contact and step length: the effect of limb length, running speed, load carrying and incline. *J. Exp. Biol.* **203**, 221-227.

**Hreljac, A.** (1993). Determinants of the gait transition speed during human locomotion: kinetic factors. *Gait Posture* **1**, 217-223.

**Hügelshofer, J.** (1982). Vergleichende Kraft- und Belastungszeit-Messungen an den Vorderhufen von gesunden und an Podotrochlose erkrankten Pferden. *Ph.D. Thesis.* University of Zurich.

**Kai, M., Aoki, O., Hiraga, A., Oki, H. and Tokuriki, M.** (2000). Use of an instrument sandwiched between the hoof and shoe to measure vertical ground reaction forces and three-dimensional acceleration at the walk, trot, and canter in horses. *Am. J. Vet. Res.* **61**, 979-985.

**Kram, R. and Dawson, T. J.** (1998). Energetics and biomechanics of locomotion by red kangaroos (*Macropus rufus*). *Comp Biochem. Physiol B* **120**, 41-49.

**Kram, R. and Taylor, C. R.** (1990). Energetics of running: a new perspective. *Nature* **346**, 265-267.

**Marey, E. J.** (1882). *La Machine Animale, Locomotion Terrestre et Aérienne.* 3rd edition. Paris: Germer Baillière et Cie.

**McGuigan, M. P. and Wilson, A. M.** (2003). The effect of gait and digital flexor muscle activation on limb compliance in the forelimb of the horse *Equus caballus*. *J. Exp. Biol.* **206**, 1325-1336.

**Merkens, H. W. and Schamhardt, H. C.** (1988a). Evaluation of equine locomotion during different degrees of experimentally induced lameness. I: Lameness model and quantification of ground reaction force patterns of the limbs. *Equine Vet. J. Suppl.* **6**, 99-106.

**Merkens, H. W. and Schamhardt, H. C.** (1988b). Evaluation of equine locomotion during different degrees of experimentally induced lameness. II: Distribution of ground reaction force patterns of the concurrently loaded limbs. *Equine Vet. J. Suppl.* **6**, 107-112.

**Merkens, H. W., Schamhardt, H. C., van Osch, G. J. and Hartman, W.**

(1993). Ground reaction force patterns of Dutch Warmbloods at the canter. *Am. J. Vet. Res.* **54**, 670-674.

**Minetti, A. E.** (1998). The biomechanics of skipping gaits: a third locomotion paradigm? *Proc. R. Soc. Lond B Biol. Sci.* **265**, 1227-1235.

**Nilsson, J. and Thorstensson, A.** (1989). Ground reaction forces at different speeds of human walking and running. *Acta Physiol. Scand.* **136**, 217-227.

**Pratt, G. W., Jr and O'Connor, J. T., Jr** (1976). Force plate studies of equine biomechanics. *Am. J. Vet. Res.* **37**, 1251-1255.

**Ratzlaff, M. H., Frame, J., Miller, J, Kimbrell, J. and Grant, B.** (1985). A new method for repetitive measurements of locomotor forces from galloping horses. In *Proceedings of the 9th Equine Nutrition and Physiology Symposium*, pp. 260-265. East Lansing, MI: Michigan State University.

**Ratzlaff, M. H., Hyde, M. L., Grant, B. D. and Wilson, P. D.** (1990). Measurement of vertical forces and temporal components of the strides of horses using instrumented shoes. *J. Equine Vet. Sci.* **10**, 23-25.

**Roepstorff, L. and Drevemo, S.** (1993). Concept of a force-measuring horseshoe. *Acta Anat.* **146**, 114-119.

**Schamhardt, H. C. and Merkens, H. W.** (1994). Objective determination of ground contact of equine limbs at the walk and trot: comparison between ground reaction forces, accelerometer data and kinematics. *Equine Vet. J. Suppl* **17**, 75-79.

**Stashak, T. S.** (2002). *Adam's Lameness in Horses*. Fifth edition. Baltimore, MD: Lippincott, Williams and Wilkins.

**Weyand, P. G., Kelly, M., Blackadar, T., Darley, J. C., Oliver, S. R., Ohlenbusch, N. E., Joffe, S. W. and Hoyt, R. W.** (2001). Ambulatory estimates of maximal aerobic power from foot–ground contact times and heart rates in running humans. *J. Appl. Physiol* **91**, 451-458.

**Wickler, S. J., Hoyt, D. F., Cogger, E. A. and Myers, G.** (2003). The energetics of the trot–gallop transition. *J. Exp. Biol.* **206**, 1557-1564.

**Willemen, M. A., Savelberg, H. H., Bruin, G. and Barneveld, A.** (1994). The effect of toe weights on linear and temporal stride characteristics of standardbred trotters. *Vet. Q.* **16(Suppl. 2)**, S97-S100.

**Wilson, A. M. and Goodship, A. E.** (1994). Exercise-induced hyperthermia as a possible mechanism for tendon degeneration. *J. Biomech.* **27**, 899-905.